

Extraction of Fault Patterns on SLS Part Surfaces Using the Karhunen-Loève Transform

Irem Y. Tumer Kristin L. Wood Ilene J. Busch-Vishniac
Graduate Research Asst. Associate Professor Professor

Mechanical Engineering Department
The University of Texas at Austin

Abstract

To gain a thorough understanding of the fault mechanisms in SLS machines, we decompose SLS profile signals into independent features using a novel tool called Karhunen-Loève (KL) transform. These individual features can then be studied separately to monitor the occurrence of fault patterns on manufactured parts and determine their nature. Analytical signals with known fault patterns, simulating profile measurement signals from SLS parts, are used to determine the suitability of the proposed method. Multi-component patterns are assumed to manifest on SLS part surfaces, resulting from faults in the machine, for example, the roller mechanism. The results of this work determine the suitability of the KL transform for condition monitoring and extraction of fault-indicating patterns.

Fault Patterns on Manufactured Parts

Detecting and quantifying faults that occur during manufacturing is necessary to ensure the efficient production of accurate parts. The field of fault detection and diagnosis in manufacturing aims at eliminating the occurrence of faults by continuously monitoring the process, detecting faults, and taking corrective action. In this paper, the focus is on monitoring the condition of surface quality. The surface is measured at regular intervals for the purpose of detecting any degradation on part surface quality. Faults or deviations in the dynamics of the manufacturing machine or its submechanisms are assumed to leave a “fingerprint” on the surface of the part being manufactured, which manifest as fault patterns. These are the fault patterns that we seek to detect, quantify, and diagnose, in order to take remedial action if necessary.

A fault is defined as the inability of a system to perform in an acceptable manner [9]. Faults typically manifest themselves as deviations in observed behavior from a set of acceptable behaviors. Fault detection is the recognition of an unacceptable behavior; and fault diagnosis is the identification of a component or set of components in the system that causes the fault [9]. As part of fault detection, analysts collect data, extract relevant features, and compare these extracted features to a specification of correct or incorrect data [5, 9].

The method of feature extraction and selection is a critical factor in detecting the correct fault-indicating features from manufacturing signals. Complex signals are best analyzed and processed using signal processing tools. In this research, we aim to develop a unified method to detect and diagnose the correct features in an accurate fashion.

The most reliable methods of fault diagnosis utilize signal processing algorithms to extract fault features. Poorly performing fault monitoring and diagnosis systems are common in industry, and they result in frequent false alarms or insensitivity to a legitimate failure condition [10]. It is often difficult to detect the proper features in the presence of random effects and nonstationarities. The

task of diagnosis is often too complex and unreliable because of errors introduced due to the careless selection of signal processing algorithms [10]. As a result, in this research, signal processing methods will be investigated to evaluate their suitability as feature extraction methods. Specifically, fault patterns on manufactured part surfaces will be analyzed to determine the character, severity, and origin of faults that result in poor surface quality.

Similarly, ongoing research aims at finding the best approach to classify the extracted features, in order to determine the existence and cause of a fault. This step typically relies on previously known limits and specifications, or previously known fault patterns. The most traditional approach to detect faulty features or patterns is to compare the observed features to previously known features. In this research, we want to develop a diagnosis method that does not rely on previous knowledge. A good example of such a case is a completely new system where there is not enough prior experience and system models for fault classification are not available. This constitutes a very difficult problem, as it requires any type of fault pattern to be recognized, quantified, and diagnosed, without prior knowledge of the expected faults.

We propose to develop a fault detection and diagnosis approach composed of signal processing tools that will detect and quantify a fault-indicating pattern (feature), regardless of the type and characteristics of the patterns and the observed signals, and that will diagnose the originating source of the fault, without relying on previous knowledge or known patterns of faults. We aim to do this in the context of monitoring and controlling part surface quality in manufacturing, specifically, in Selective Laser Sintering [12].

To satisfy our research goals, we propose a five-step approach, shown schematically in Figure 1. The main two general portions of this approach consist of feature extraction and quantification and

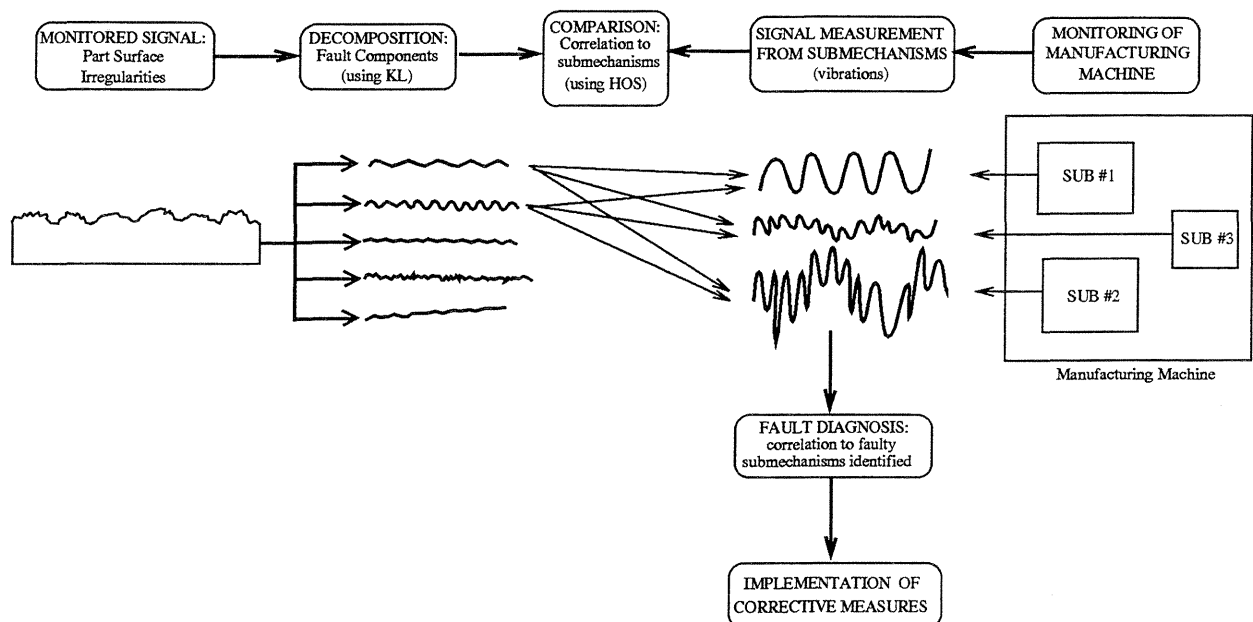


Figure 1: Feature Extraction and Fault Diagnosis Approach.

feature comparison for diagnosis. To obtain a decorrelated decomposition of the measured signal, we need to apply a mathematical transformation to the signal [1, 14]. The Fourier transform is such a tool, resulting in a decomposition into different frequency components based on sines and cosines as basis vectors. However, the decomposition is not accurate in the presence of nonstationary features.

An alternative is the Karhunen-Loève (KL) transform, an orthogonal transform which decomposes the signals into decorrelated components in the form of a few empirical basis functions that contain the majority of the variance in the original data. The most common application of this transform is to detect dominant features in order to reconstruct original signals with lower dimensionality. Recent applications include recognition of faces in vision and turbulent structures in fluids [3, 6, 8]. We want to use this tool in detecting features in manufacturing signals, specifically, surface profiles [11]. Our main purpose is to extract individual patterns and study their characteristics to determine whether they correspond to significant faults, and use these patterns to determine their origin.

This paper focuses on the first two steps. In particular, we investigate the suitability of the Karhunen-Loève transform to provide a proper decomposition leading to accurate fault detection, quantification, and monitoring. The following sections describe the theory and motivation of the KL transform and investigate its suitability based on analytical signals which model multi-component signals and the occurrence of faults.

Karhunen-Loève Transform

Orthogonal transforms, and, in particular, the optimal Karhunen-Loève transform (KL), otherwise known as the Principal Components Analysis in the statistical literature, are used in a variety of signal processing applications [1, 2, 3, 6, 8, 15]. However, they have never been used for the purposes of fault detection and diagnosis, or for the purposes of detecting and quantifying faults on manufactured part surfaces. In this work, we extend the KL transform to the extraction of physical patterns from surface signals; the purpose is to decompose multi-component signals into individual patterns and study their characteristics in order to determine the occurrence, severity, and shape of each fault. We want to assure that any pattern, including stationary and nonstationary, can be detected and extracted using the KL transform. This information will later be used to diagnose the origin of each individual fault.

The KL transform presents a great advantage when investigating the occurrence of faults, especially when the shape of the fault patterns are not known in advance. Orthogonal transforms provide a decomposition of the signal into its high-energy content basis functions, leading to an accurate decomposition picture in the time-domain [1, 7]. Because the KL method decomposes signals into empirically determined basis functions, rather than pre-defined sines and cosines, any fault pattern, including stationary and nonstationary patterns, can be detected in theory using this transform.

Theory and Mathematics

In the context of surface profile characterization, the signal being monitored is the surface profile of an SLS part. A total of M “snapshots” are assumed to be collected at regular intervals, with N points each, to allow for a continual monitoring of the state of operation.

We first compute the mean vector $\vec{X}_{ave} = \frac{1}{M} \sum^m \vec{X}_m$ over the total of M samples collected from the profile; then the deviation or departure $\vec{y}_m = \vec{X}_m - \vec{X}_{ave}$ of each sample signal from the mean is computed. The mean is removed to simplify the mathematical derivation of the covariances [4]. Next, the covariance matrix is computed as follows:

$$\vec{C} = \frac{1}{M} \sum_{m=1}^M \vec{y}_m [\vec{y}_m]^T \quad (1)$$

The eigenvectors of \vec{C} are the basis functions \vec{u}_i , computed from:

$$\vec{C}\vec{u}_i = \lambda_i\vec{u}_i \quad (2)$$

The eigenvalues λ_i are ordered and the relevant features are selected by choosing the first $n < N$ dominant eigenvalues from the set of solutions, following the feature selection criterion used in the literature (about 90% of the total energy is sufficient for reconstruction [3]). The coefficients a_i are computed by projecting each sample vector deviation \vec{y}_m^- onto the basis vectors \vec{u}_i from:

$$a_i = [\vec{y}_m^-]^T \vec{u}_i \quad (3)$$

For each deviation \vec{y}_m^- , there are $i = 1 \dots n$ coefficients, where n is the number of principal eigenvectors; there are a total of $m = 1 \dots M$ deviations (snapshots). From another point of view, for each principal eigenvector \vec{u}_i , $i = 1 \dots n$, there are $m = 1 \dots M$ coefficients. The collection of these M coefficients for each eigenvector is called the coefficient vector; hence, there are as many coefficient vectors as there are eigenvectors. Each original sample vector \vec{X}_m is then reconstructed with lower dimensionality by adding this linear combination to the sample mean:

$$\vec{X}_m = \vec{X}_{ave} + \sum_{i=1}^n a_i \vec{u}_i \quad (4)$$

Simulations using Analytical Signals

In this paper, faults are simulated in the context of parts from a Selective Laser Sintering machine. The roller in the SLS machine is responsible for depositing an even layer of powder on the powder bed [12, 13]. The quality (“evenness”) of the surface of the top layer of powder will determine, in part, the surface quality of the final manufactured part. In a previous paper, the authors have shown that, with certain types of powder, the roller leaves “chatter marks” on the surfaces of SLS parts [12, 13]. Any undesirable changes in the dynamics of the roller will result in a change in the surface quality of the part being manufactured. It is changes such as these that we want to be able to detect using the KL transform.

In order to test the suitability and limitations of the KL transform, we use analytical signals in which the fault patterns are known. This assures the accuracy of our results, since we know exactly what fault patterns the decomposition should provide, and when each type of fault pattern occurs. We first simulate cases where different faults occur during a manufacturing process, and compare these cases to the normal state of operation. With these simulations, we also want to assure that multicomponent signals are decomposed accurately, whether the components are deterministic, stochastic, stationary, or nonstationary. Deterministic and stationary changes are introduced, as well as nonstationary changes over the entire monitored profile.

The “normal” state of operation is assumed to produce a multicomponent signal with 2 sinusoids, in the form of $A_1 \sin(F_1 j) + A_2 \sin(F_2 j)$, one high frequency ($F_1 = 0.9 \text{ rad/sec}$), small amplitude ($A_1 = 1 \text{ mm}$), and the other low frequency ($F_2 = 0.2 \text{ rad/sec}$) and large amplitude ($A_2 = 2 \text{ mm}$), plus random (Gaussian) noise (zero mean and low variance of 0.09). This situation illustrates a typical operation state, in which rotating components, such as the SLS roller, introduce a fundamental sinusoidal pattern, plus a harmonic, accompanied with random noise from the machine operation or other conditions, such as the surface texture of the roller. Faults, such as bearing wear or misalignment, introduce either additional harmonics, or a change in the magnitude

Ind.	Normal	Abnormal 1a	Abnormal 1b	Abnormal 2a	Abnormal 2b	Abnormal 3	Abnormal 4
1	255.45	633.47	6938.42	1006.66	6232.03	1037.00	829.55
2	240.15	530.83	5738.31	956.76	5938.75	954.40	685.45
3	74.01	240.76	245.89	72.23	70.81	618.54	89.81
4	55.62	235.70	235.65	57.30	57.61	485.89	84.81
5	2.68	2.81	2.86	2.59	2.75	2.66	52.88
6	2.58	2.39	2.62	2.27	2.21	2.24	26.23
7	2.25	2.25	2.39	2.25	2.08	2.12	2.81
8	2.14	2.00	2.06	2.00	1.95	1.98	2.29
9	2.00	1.73	1.79	1.97	1.64	1.74	1.97
10	0.00	0.00	0.00	0.00	0.00	0.00	0.00

Table 1: Eigenvalues: Normal State vs. Abnormal States

of the fundamental frequency component. In addition, offsets or linear trends may be introduced as a result of misalignment in the non-rotating elements. In the following, These abnormal cases, as well as other nonstationary faults, are simulated and compared to the normal state of operation.

In the following, the “eigenprofiles” represent the principal basis patterns on the entire surface being monitored. Snapshots are collected at regular intervals to monitor the condition of the surface being manufactured. Significant “eigenprofiles” are derived from a covariance matrix to provide the shape of the dominant patterns on surface profiles; the eigenvalue corresponding to each eigenprofile indicates the effectiveness of each feature to represent the original profile. The features are the coefficient vectors corresponding to each eigenvalue; these indicate any change in amplitude of a dominant eigenprofile along the snapshots collected in time or in space, corresponding to the weight of each basis eigenprofile in each snapshot. The variance of the coefficient vectors follows the magnitude of the eigenvalue. There are as many coefficient vectors as there are dominant eigenprofiles. The coefficient vector contains M points, indicating the change over M profile snapshots.

Stationary Changes in Deterministic Components

In the first set of simulations, the normal state of operation is assumed to produce a multi-component signal with 2 sinusoids and random (Gaussian) noise. Ten snapshots are assumed to be collected over the entire profile; each snapshot has 256 sample points. The following set of simulations test the effect of stationary changes in the deterministic components.

Abnormal States 1a and 1b

In the first case, the high frequency component of the signal increases in magnitude, while the second component remains unchanged. Abnormal states 1a and 1b represent two different magnitudes. We are investigating whether changes in the amplitude of one of the sinusoidal components of the multi-component signal can be detected with the KL transform. This might, for example, simulate the case when a sinusoidal pattern on the SLS surfaces, caused by roller chatter [12], exceeds its normal limits in magnitude, thus reducing the surface precision and accuracy; remedial action will have to be taken to diagnose the cause of this increase.

The eigenvalues from abnormal states 1a and 1b, compared to the normal state, are shown in Table 1. The first observation is that, for the normal state of operation, the multi-component signal is decomposed into 4 significant eigenvalues, summing to 98% of the total energy in the signal. The first two eigenvalues (#1,#2) correspond to low-frequency sinusoidal eigenprofiles, while the next two eigenvalues (#3,#4) correspond to high-frequency sinusoidal eigenprofiles.

For abnormal states 1a and 1b, we also obtain 4 principal eigenvalues and eigenprofiles. As shown in Table 1, when we increase the magnitude of the high-frequency component of our original signal, we notice that the eigenvalues corresponding to the high-frequency component increase in magnitude. The eigenvalues corresponding to the low-frequency component remain approximately the same as in the normal state of operation.

These trends are more easily noticeable when we study the shape of the eigenprofiles and the corresponding coefficient vectors. The first four eigenvectors from abnormal states 1a and 1b, compared to the normal state, are shown in Figure 2. The corresponding coefficient vectors are

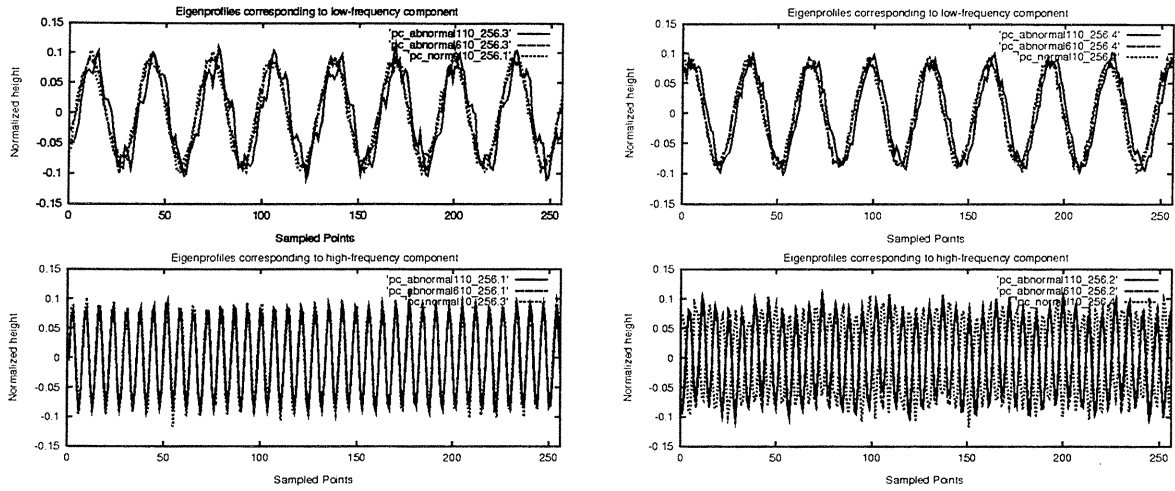


Figure 2: Principal Eigenprofiles from Normal vs. Abnormal States 1a & 1b

shown in Figure 3. Notice that the shape of the eigenprofiles are approximately the same for the

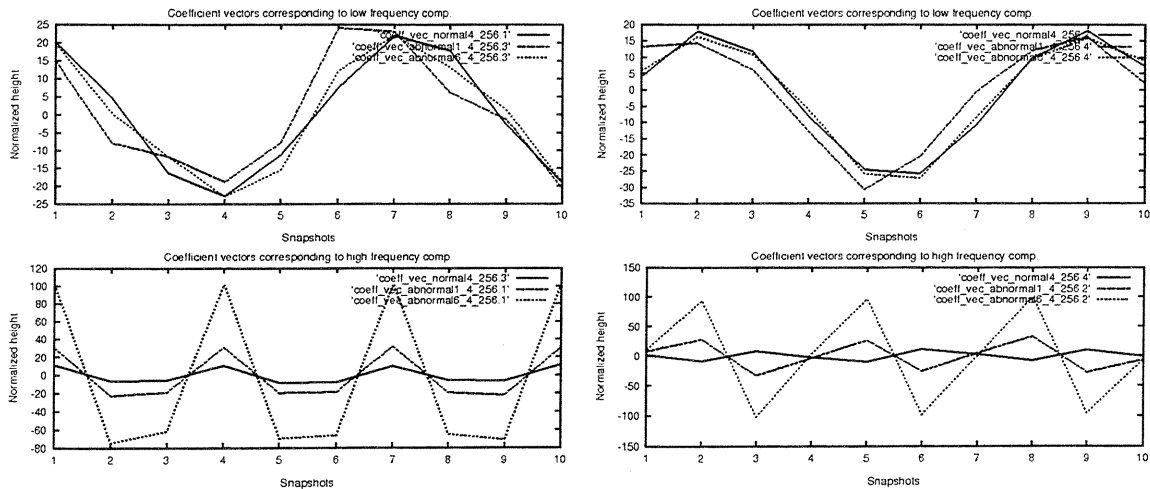


Figure 3: Coefficient Vectors: Normal vs. Abnormal States 1a & 1b.

normal state, and abnormal states 1a and 1b. This result is expected since we are only changing the magnitude of the high-frequency sinusoidal component, and not the frequency. The change in magnitude is detected using the coefficient vectors. Also notice that, the coefficient vectors corresponding to the high-frequency component show a steady increase in magnitude, On the other

hand, the coefficient vectors corresponding to the low-frequency component show no detectable change. The change in magnitude is successfully detected by monitoring the coefficient vectors.

Abnormal States 2a and 2b

In this case, we simulate an increase in the magnitude of the low-frequency component. The simulation results show that the eigenvalues corresponding to the low-frequency component increase in magnitude, as the magnitude of the low-frequency sinusoidal component increases. The eigenvalues corresponding to the high-frequency components remain approximately the same in magnitude as in the normal state (see Table 1).

In addition, the first four eigenprofiles from abnormal states 2a and 2b, are the approximately the same as in the normal state and in abnormal states 1a and 1b. This result is not surprising since we are not changing the shape of the pattern, but only the magnitude. The change in magnitude is properly detected with the corresponding coefficient vectors. In this case, the coefficient vectors corresponding to the high-frequency component remain unchanged, while the coefficient vectors corresponding to the low-frequency component show a steady increase in magnitude. Once again, the coefficient vectors can be monitored to detect the change in magnitude of any frequency component in the measured signal. In addition to these results, further simulation shows that, when both the high-frequency and the low-frequency components of the multi-component signal are increased in magnitude, the changes in magnitude are again successfully detected by monitoring the coefficient vectors (abnormal state 3, Table 1).

Abnormal State 4

Finally, we investigate whether the KL transform detects the occurrence of an unexpected fault. The fault, in this case, is introduced in the form of an additional frequency component. This simulates the case where the bearing of the roller in the SLS machine undergoes wear, hence introducing a harmonic, in addition to the fundamental frequency component. The first two sinusoidal components are the same as the normal state of operation; a third frequency component is added (abnormal state 4). In this case, the addition of a third frequency component introduces an additional set of eigenvalues (see Table 1). Therefore, the occurrence of an additional frequency component can be detected by monitoring the number of significant eigenvalues. The accuracy of this case needs to be investigated further.

Nonstationary Changes

The second set of simulations tests the effect of introducing sudden and/or gradual nonstationary changes to the monitored signal. These cases simulate the occurrence of faults after a certain point in time, introducing a nonstationary pattern over the monitored signal. Four cases are simulated, presented next. The eigenvalues for each of these cases, compared to the normal state of operation, are presented in Table 2.

Case 1

In the first case, signals from the normal state of operation are assumed to have a change in the mean offset after a certain period of time, hence introducing a nonstationary change in the signal that must be detected during monitoring; the first ten snapshots indicate normal status, while the next ten snapshots indicate an offset. This situation, for example, simulates a sudden change

Index	Normal	Case 1	Case 2	Case 3	Case 4
1	255.45	1602.78	3243.81	2253.35	346191.37
2	240.15	254.08	3191.27	2239.68	254.37
3	74.01	239.45	71.59	1397.22	240.01
4	55.62	69.86	56.26	69.79	69.38
5	2.68	55.23	1.52	56.32	56.66
6	2.58	1.66	1.49	1.20	2.36
7	2.25	1.41	1.36	1.08	2.21
8	2.14	1.32	1.33	1.05	2.11
9	2.00	1.24	1.26	1.01	1.92
10	0.00	1.22	1.22	0.92	0.03

Table 2: Results: Eigenvalues for Normal State vs. Cases 1 through 4

in the vertical position of the SLS part while it is being formed, caused by the residue deposited on the roller mechanism. As shown in Table 2, this fault manifests itself as an added principal eigenprofile, with a relatively large eigenvalue; the remaining eigenvalues are approximately the same as the normal state of operation. The simulation results show that the first eigenprofile resembles a straight line when plotted with the remaining sinusoidal eigenprofiles. In addition, the coefficient vector corresponding to the first eigenvalue shows the change in the mean offset very clearly, after the tenth snapshot, as shown in Figure 4. As a result, this additional pattern, defined by a straight line, can be detected by monitoring the occurrence of a fifth eigenprofile, while its significance can be evaluated by monitoring the shape of the coefficient vector. Note that no change is observed in the remaining eigenprofiles or coefficient vectors, when compared with the normal state of operation.

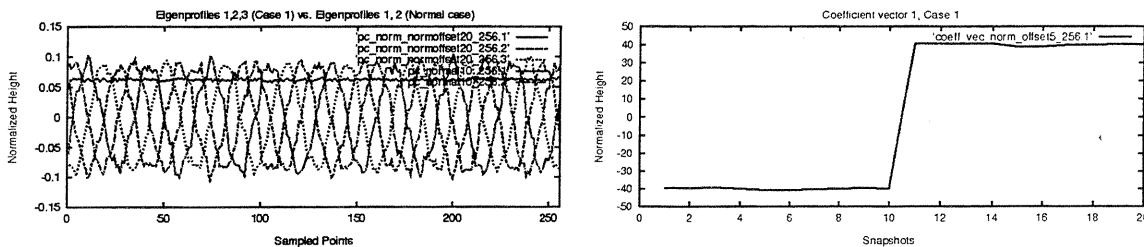


Figure 4: Principal Eigenprofiles and Coefficient Vector for Case 1.

Case 2

In this case, a situation similar to abnormal states #2 and #5 occurs, where the low-frequency component changes in magnitude, while the high-frequency component remains the same. We collect a total of twenty snapshots; a change occurs during the course of monitoring the signal, hence introducing a nonstationary change in the signal, after the tenth snapshot. The results show that, while the eigenprofiles remain the same as in the normal state of operation, the coefficient vectors corresponding to the low-frequency eigenprofiles increase in magnitude after the tenth snapshot, where the nonstationary change occurs (Figure 5). As expected, no change is observed in the high-frequency coefficient vectors (Figure 5). Also notice the increase in the eigenvalues for the first two eigenprofiles, while the eigenvalues for the next two eigenprofiles are approximately the same as the normal state of operation, as shown in Table 2.

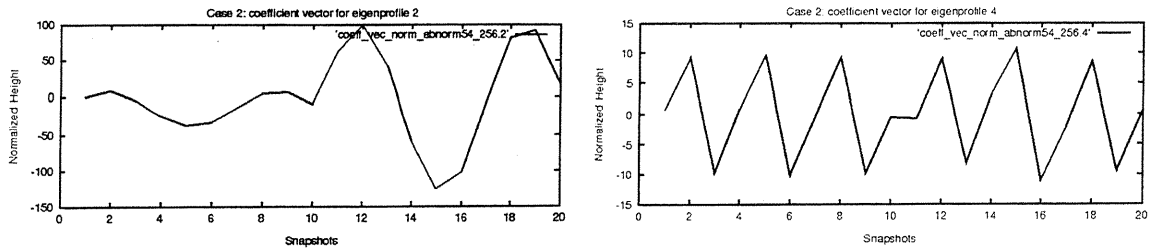


Figure 5: Principal Eigenprofiles from Normal State vs. Case 2.

Case 3

When both Case 1 and Case 2 take place, i.e., first the magnitude of the low-frequency sinusoidal component increases (after the tenth snapshot), then, a change in the mean offset is observed (after the twentieth snapshot), result show similar trends; in this case, we collect a total of thirty snapshots to observe both types of changes occurring at different points in time. A fifth eigenvalue/eigenprofile is observed, reflecting the change in the offset value, plus an increase in the first two eigenvalues, corresponding to the low-frequency eigenprofiles; the last two eigenvalues remain approximately the same as in the normal state of operation (Table 2, Case 3). In addition, as expected, the coefficient vectors corresponding to the low-frequency eigenprofiles show a change in magnitude after the tenth snapshot, and return to their original normal state after the twentieth snapshot. The coefficient vector corresponding to the third eigenprofile indicates the change in the offset value after the twentieth snapshot, while the coefficient vectors corresponding to the last two eigenprofiles show no change.

Case 4

In the final case, the normal state of operation is interrupted by the addition of a linear trend with a positive slope. This simulates, for example, a change in the table or powder bed slope while the SLS part is being manufactured. The results show the addition of a fifth eigenvalue (Table 2, Case 4) of large magnitude, while the remaining four eigenvalues are approximately the same as the normal state of operation. The first three eigenprofiles and the coefficient vector corresponding to the first eigenprofile are shown in Figure 6. As expected, the first eigenprofile represents a

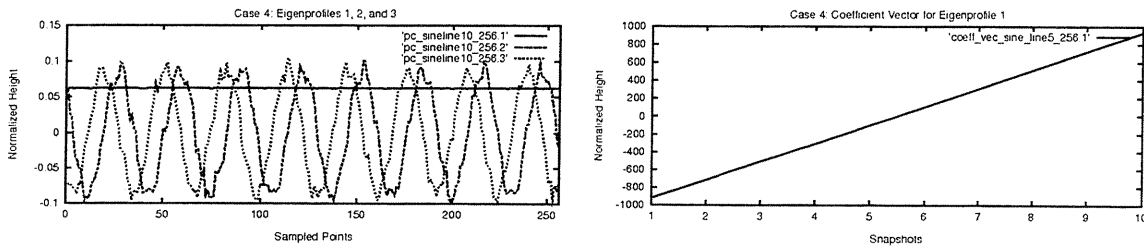


Figure 6: Principal Eigenprofiles and Coefficient Vectors for Case 4.

straight line as the basis vector, while the corresponding coefficient vector indicates the change in the magnitude of that principal eigenprofile, reflecting the slope in the linear trend.

Conclusions from the Simulation Results

The simulation results show that the KL transform presents a good potential for detecting, extracting, and monitoring fault patterns on surface profiles. First, the KL transform successfully decomposes the signal into its basis patterns (eigenprofiles). Changes in the magnitudes of these basis patterns are successfully reflected in the corresponding coefficient vectors. The introduction of additional patterns are also detected as additional basis patterns. For example, in case 1, the KL transform successfully decomposes the signal into its individual patterns, i.e., 2 sinusoids and a straight line. Monitoring is done by detecting a fifth eigenprofile and studying the change in the corresponding coefficient vector. In addition, the nonstationary change in the offset level is reflected in the relevant coefficient vector, hence allowing the effective monitoring of this nonstationary change in the normal state of operation. In case 2, the sudden change in the magnitude of the sinusoidal patterns is successfully reflected in the relevant coefficient vectors, while no additional patterns are extracted. In case 4, the KL transform extracts the additional basis pattern, represented as a straight line, and detects the introduction of a linear trend, which is reflected in the corresponding coefficient vectors as a linear increase in magnitude over the set of snapshots. Further simulations are necessary to assure that nonstationary patterns over snapshots (as opposed to patterns over the entire signal) are also detectable with this method. An example is a set of linear trends with differing slopes over each snapshot.

Conclusions and Future Work

This paper presents a study of the suitability of an orthogonal transform, namely the Karhunen-Loève transform, in decomposing signals measured from SLS part surfaces. We show that the KL transform can be used to detect stationary as well as nonstationary patterns, providing an accurate decomposition of multi-component signals. In addition, we show that the eigenprofiles and coefficient vectors derived using the KL transform can be used to effectively monitor and detect the occurrence of faults on measured SLS surface signals.

Stationary changes, including changes in the magnitudes of one or more sinusoidal components, are reflected as changes in the corresponding coefficient vectors. The introduction of an additional frequency component is reflected by an increase in the number of principal eigenvalues and eigenprofiles. Nonstationary changes in the normal state of operation, including a change in the mean offset level, and a change in the slope of the part surface, are reflected by the introduction of additional eigenprofiles and corresponding changes in the coefficient vectors. A sudden change in the magnitude of a sinusoidal pattern is reflected by an accurate change in the corresponding coefficient vector. As a result, the KL transform is shown to be a proper tool in extracting the relevant features and monitoring stationary and nonstationary changes in the normal state of operation, for those cases simulated in this paper. Further mathematical proof of these results will follow.

In addition to the work presented in this paper, the authors are currently simulating other fault components, such as transients, and other nonstationary fault components, such as a saw-tooth shaped pattern. Other transforms such as the wavelet transforms and higher-order spectral transforms are also being investigated as potential candidates to provide an effective and accurate decomposition of multi-component signals. The results of this work will be used to develop an accurate fault detection and diagnosis method to assure the quality of surfaces from manufacturing machines.

Acknowledgements

This material is based on work supported, in part, by The National Science Foundation, Grant No. DDM-9111372; an NSF Presidential Young Investigator Award; by a research grant from TARP; plus research grants from Ford Motor Company, Texas Instruments, and Desktop Manufacturing Inc., and the June and Gene Gillis Endowed Faculty Fellowship in Manufacturing.

References

- [1] A.N. Akansu and R.A. Haddad. *Multiresolution Signal Decomposition: Transforms, Subbands, Wavelets*. Academic Press, Inc., San Diego, Ca, 1992.
- [2] V. R. Algazi, K. L. Brown, and M. J. Ready. Transform representation of the spectra of acoustic speech segments with applications, part I: General approach and application to speech recognition. *IEEE Transactions on Speech and Audio Processing*, 1(2):180–195, April 1993.
- [3] K.S. Ball, L. Sirovich, and L.R. Keefe. Dynamical eigenfunction decomposition of turbulent channel flow. *International Journal for Numerical Methods in Fluids*, 12:585–604, 1991.
- [4] J. S. Bendat and A. G. Piersol. *Random Data: Analysis and Measurement Procedures*. John Wiley & Sons, New York, NY, 1986.
- [5] S. D. Eppinger, C. D. Huber, and V. H. Pham. A methodology for manufacturing process signature analysis. *Journal of Manufacturing Systems*, 14(1):20–34, 1995.
- [6] K. Fukunaga. *Introduction to Statistical Pattern Recognition*. Academic Press, New York, NY, 1972.
- [7] W. Kozek. Matched generalized gabor expansion of nonstationary processes. In *The Twenty Seventh Asilomar Conference on Signals, Systems, & Computers*, volume 1, pages 499–503, 1993.
- [8] L. Sirovich and L.R. Keefe. Low-dimensional procedure for the characterization of human faces. *Journal of the Optical Society of America*, 4(3):519–524, March 1987.
- [9] J. Sottile and L. E. Holloway. An overview of fault monitoring and diagnosis in mining equipment. *IEEE Transactions on Industry Applications*, 30(5):1326–1332, September/October 1994.
- [10] S. Spiewak. A predictive monitoring and diagnosis system for manufacturing. *Annals of the CIRP: manufacturing technology*, 40(1):401–404, 1991.
- [11] I.Y. Tumer, R.S. Srinivasan, and K.L. Wood. Investigation of characteristic measures for the analysis and synthesis of precision-machined surfaces. *Journal of Manufacturing Systems*, 14(5):378–392, September/October 1995.
- [12] I.Y. Tumer, D.C. Thompson, R.H. Crawford, and K.L. Wood. Surface characterization of polycarbonate parts from selective laser sintering. In *SFF Symposium Proceedings*, pages 181–188. The University of Texas at Austin, August 1995.
- [13] I.Y. Tumer, D.C. Thompson, K.L. Wood, and R.H. Crawford. Characterization of surface fault patterns with applicaiton to a layered manufacturing process. *Submitted for review to the Journal of Manufacturing Systems, Special Issue in Layered Manufacturing Systems*, February 1996.
- [14] D.J. Whitehouse. *Handbook of Surface Metrology*. Institute of Physics Publishing, Bristol, UK, 1994.
- [15] S. A. Zahorian and M. Rothenberg. Principal-components analysis for low-redundancy encoding of speech spectra. *Journal of the Acoustical Society of America*, 69(3):519–524, March 1981.

